Eur. J. Mineral.
2016, **28**, 1005–1017
Published online 14 June 2016

Magnesiovoltaite, $K_2Mg_5Fe^{3+}{}_3Al(SO_4)_{12}\cdot 18H_2O$, a new mineral from the Alcaparrosa mine, Antofagasta region, Chile

NIKITA V. CHUKANOV[1,*], SERGEY M. AKSENOV[2,3], RAMIZA K. RASTSVETAEVA[4], GERHARD MÖHN[5], VYACHESLAV S. RUSAKOV[6], IGOR V. PEKOV[7], RICARDO SCHOLZ[8], TATIANA A. EREMINA[7], DMITRIY I. BELAKOVSKIY[9] and JOACHIM A. LORENZ[10]

[1] Institute of Problems of Chemical Physics, Russian Academy of Sciences, Chernogolovka, Moscow region, 142432 Russia
*Corresponding author, e-mail: chukanov@icp.ac.ru.
[2] Dept. of Crystallography, St Petersburg State University, University Embankment 7/9, St Petersburg, 199034 Russia
[3] Nesmeyanov Institute of Organoelement Compounds, Russian Academy of Sciences, GSP-1, Vavilova St. 28, Moscow, V-334, 119991 Russia
[4] Institute of Crystallography, Russian Academy of Sciences, 59 Leninskiy Prospekt, Moscow, 117333 Russia
[5] Dr J. Wittemannstrasse 5, 65527 Niedernhausen, Germany
[6] Faculty of Physics, Moscow State University, Vorobievy Gory, Moscow, 119991 Russia
[7] Faculty of Geology, Moscow State University, Vorobievy Gory, Moscow, 119991 Russia
[8] Universidade Federal de Ouro Preto (UFOP), Escola de Minas, Departamento de Geologia, Campus Morro do Cruzeiro, 35400-000, Ouro Preto, MG, Brazil
[9] Fersman Mineralogical Museum of Russian Academy of Sciences, Leninskiy Prospekt 18-2, Moscow, 119071 Russia
[10] Graslitzer Strasse 5, 63791 Karlstein, Germany

Abstract: Magnesiovoltaite, a new voltaite-group mineral, was discovered in the Alcaparrosa mine, Cerro Alcaparrosa, El Loa province, Antofagasta region, Chile, in two associations, one of which includes coquimbite, tamarugite, alum-(Na), rhomboclase, yavapaiite, voltaite and opal, and the other one is botryogen, opal, tamarugite, alum-(K), pickeringite, magnesiocopiapite, and jarosite. Magnesiovoltaite forms yellow, brownish-yellow or pale yellowish-greenish isometric crystals up to 2 mm across. The main crystal forms are {111} and {100}; the subordinate forms are {110} and {211}. The new mineral is brittle, with subconchoidal fracture; cleavage is not observed. Mohs' hardness is 2½. D_{meas} = 2.51(2) g/cm^3, D_{calc} = 2.506 g/cm^3. Magnesiovoltaite is optically anomalously anisotropic, uniaxial with ε = 1.584(2) and ω = 1.588(2), or biaxial (–) with α = 1.584(2), β = 1.587(2), and γ = 1.588 (2). Possible causes of the optical anomalies are discussed. The infrared spectrum is given. The chemical composition is (EDS-mode electron microprobe, all iron is considered as Fe^{3+} in accordance with Mössbauer data, H_2O by gas chromatography of ignition products, wt. %): Na_2O 0.13, K_2O 4.64, MgO 9.13, MnO 1.73, ZnO 0.84, Al_2O_3 2.47, Fe_2O_3 13.36, SO_3 50.83, H_2O 17.6, total 100.73. The empirical formula based on 66 O atoms per formula unit (*apfu*) is $(K_{1.85}Na_{0.08})(Mg_{4.25}Mn_{0.46}Zn_{0.14})Fe^{3+}{}_{3.14}Al_{0.91}(SO_4)_{11.91}(H_2O)_{18.325}O_{0.035}$. The simplified formula is $K_2Mg_5Fe^{3+}{}_3Al(SO_4)_{12}\cdot 18H_2O$. The crystal structure has been refined to R = 3.2% using 1147 unique reflections with $I > 2\sigma(I)$. Magnesiovoltaite is cubic, *Fd–3c*, a = 27.161(1) Å, V = 20038(2) Å^3, and Z = 16. Magnesiovoltaite is isostructural with other cubic voltaite-group minerals. The strongest lines of the powder X-ray diffraction pattern [d, Å (I, %) (*hkl*)] are: 9.56 (29) (022), 6.77 (37) (004), 5.53 (61) (224), 3.532 (68) (137), 3.392 (100) (008), 3.034 (45) (048), 2.845 (30) (139). The type material is deposited in the collections of the Fersman Mineralogical Museum of the Russian Academy of Sciences, Moscow, Russia.

Key-words: magnesiovoltaite; new mineral; sulfate; voltaite group; crystal structure; oxidation zone; Alcaparrosa mine; Chile.

Introduction

The new mineral magnesiovoltaite described in this paper was first found in January 2013 by one of the authors (G.M.) in two mining workings belonging to the abandoned Alcaparrosa sulfate mine and located on the north side of Cerro Alcaparrosa, about 3 km southwest of the railroad station of Cerritos Bayos, Calama, El Loa province, Antofagasta region, Chile. Additional material was collected at the same locality in January 2016.

The Alcaparrosa polymetallic sulfide deposit consists of a series of iron sulfate veins and lenses of varying strikes and

DOI: 10.1127/ejm/2016/0028-2565
0935-1221/16/0028-2565 $ 5.85

dips. The deposit is hosted in volcanic rocks of the Punta del Cobre Formation composed mainly of massive andesitic and dacitic rocks (Marschik & Fontboté, 2001). It represents oxidized portions of pyritic masses formed close to the surface that have later been subjected to oxidation under increasingly arid conditions of the Atacama Desert, which is one of the driest areas on Earth (Bandy, 1938).

Magnesiovoltaite occurs in two mineral assemblages. In the first one it forms crystals growing on coquimbite; other associated minerals are tamarugite, alum-(Na), rhomboclase, yavapaiite, voltaite and opal. The presence of coquimbite in close association with magnesiovoltaite indicates that the paragenesis was formed under hyperacidic conditions (Buckby *et al.*, 2003; Romero *et al.*, 2006). In the second assemblage yellow crystals of magnesiovoltaite are overgrowing a matrix mainly consisting of botryogen and opal; other associated minerals there are tamarugite, alum-(K), pickeringite, magnesiocopiapite, and jarosite or natrojarosite. In both assemblages magnesiovoltaite is one of the latest minerals crystallized in cavities within aggregates of supergene minerals containing minor relics of a decomposed host rock (quartz, plagioclase) and a clay mineral. In the first association green-black Mg-poor voltaite is embedded in a matrix consisting of coquimbite and rhomboclase whereas magnesiovoltaite overgrows these minerals. Some crystals of the new mineral are zoned: the core is more Fe-rich and Mg-depleted. Thus, the Mg:Fe^{2+} ratio (for details see below) in voltaite-group minerals formed in this assemblage increases from their earlier generations to later ones.

The new mineral is named as an analogue of voltaite and zincovoltaite with Mg dominant at the *M*1 site. Magnesiovoltaite and its name have been approved by the IMA Commission on New Minerals, Nomenclature and Classification (IMA no. 2015-095). The type specimens are deposited in the collections of the Fersman Mineralogical Museum of the Russian Academy of Sciences, Moscow, Russia, with the registration numbers 4780/1 (fragment of the holotype) and 4780/2 (cotype).

General appearance and physical properties

Magnesiovoltaite occurs as transparent amber-yellow to brownish-yellow or pale yellow to pale yellowish-greenish, sometimes almost colourless isometric crystals up to 2 mm across (Figs. 1 and 2) in cavities of aggregates of other sulfate minerals, mainly coquimbite, rhomboclase and tamarugite. Some crystals are concentrically zoned, with darker green-grey core and pale yellowish-greenish peripheral parts enriched in Mg as compared to core. The main crystal forms are {111}, {100} and {110}. On some crystals {211} faces are also observed. Idealized drawings of magnesiovoltaite crystals are shown in Fig. 3: a – e are typical combinations of forms and f – h are rarer ones. Some crystals are distorted. For example, a crystal shaped by the faces {111}, {110}, {100} and minor {211} that simulates trigonal quartz-like form is shown in Fig. 1a. Magnesiovoltaite is brittle, has a Mohs' hardness of 2½ and a subconchoidal fracture. Neither cleavage nor parting is observed. The density measured by flotation in heavy liquids (diiodomethane-ether mixtures) is 2.51(2) g/cm^3. Densities of the liquids have been measured using a density bottle. The density calculated using the empirical formula is 2.506 g/cm^3. The new mineral is non-fluorescent under short- and long-wave UV light.

The yellow transparent crystals of magnesiovoltaite are colourless in transmitted light with λ = 589 nm, non-pleochroic and, despite the cubic symmetry, show quite noticeable anisotropy. For some grains irregular mosaic or wavy extinction is observed. The biggest grains often show conoscopic figures of a negative uniaxial crystal with ε = 1.584(2) and ω = 1.588(2). Some smallest fragments show the picture of a negative biaxial mineral with α = 1.584(2), β = 1.587(2), and γ = 1.588(2). For such grains weak to medium dispersion of optical axes was observed ($r > v$). Due to the small sizes of such fragments we were unable to measure $2V$; $2V_{calc}$ = 60°. Possible causes of the optical anomalies are discussed below.

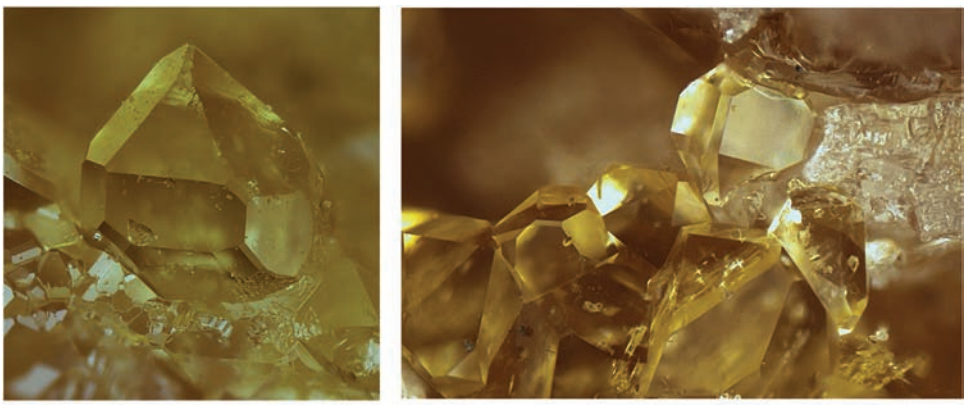

(a) (b)

Figs. 1. Crystals of magnesiovoltaite. Field of view 0.46 × 0.46 mm (a) and 0.7 × 1.0 mm (b). Photograph: M. Burkhardt. (online version in colour)

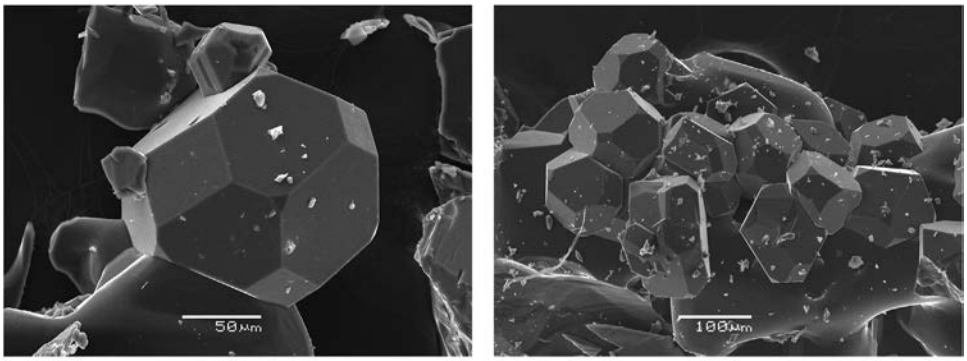

(a) (b)

Figs. 2. Typical crystals of magnesiovoltaite on tamarugite. Scanning electron microscope image, secondary electrons. (online version in colour)

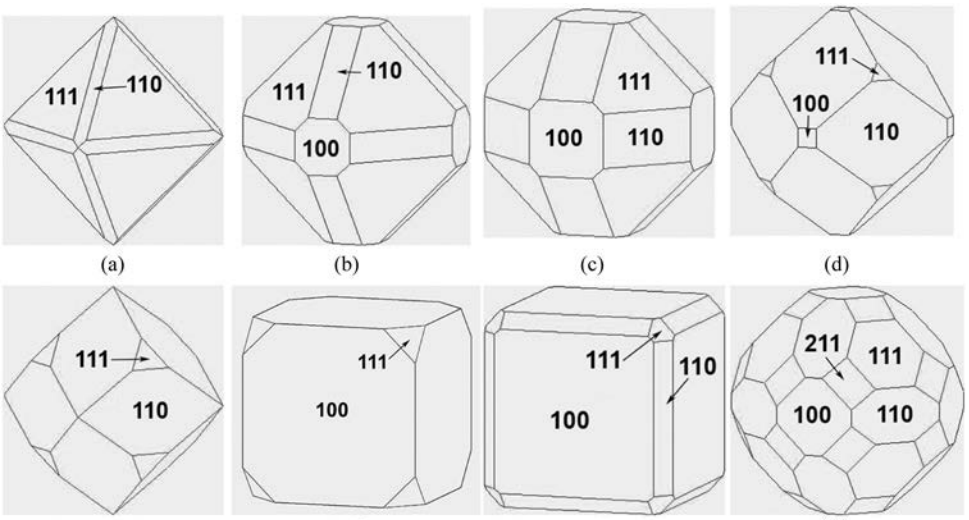

(a) (b) (c) (d)

(e) (f) (g) (h)

Fig. 3. Idealized crystals of magnesiovoltaite.

Infrared spectroscopy

In order to obtain infrared (IR) absorption spectra, powdered samples have been mixed with dried KBr, pelletized, and analyzed using an ALPHA FTIR spectrometer (Bruker Optics) with a resolution of 4 cm^{-1} and 16 scans accumulated (Fig. 4). The IR spectrum of an analogous pellet of pure KBr was used as a reference.

Wavenumbers of absorption bands in the IR spectrum of magnesiovoltaite (Fig. 4a) and their assignments (cm^{-1}; s – strong band, w – weak band, sh – shoulder) are: 3565sh, 3480sh, 3441, 3134, (3070sh) (O–H stretching vibrations of H_2O molecules), 2496w (O–H stretching vibrations of acid sulfate groups HSO_4^- formed as a result of reversible proton transfer $SO_4^{2-} + H_2O \leftrightarrow HSO_4^- + OH^-$; the low intensity of this band indicates that the dynamic chemical equilibrium is strongly shifted to the left), 1684w, 1640sh, 1624 (bending vibrations of H_2O molecules), 1168s, 1133s, 1067s [$\nu_3(F_2)$ – asymmetric stretching vibrations of SO_4^{2-} anions], 1011s, 995sh [$\nu_1(A_1)$ – symmetric stretching vibrations of SO_4^{2-} anions], 876w, 718sh (possibly, $M\cdots$O–H bending vibrations combined with overtones of M···O stretching vibrations, where $M = Fe^{3+}$ and Mg, respectively), 660sh, 629, 596 [$\nu_4(F_2)$ – bending vibrations of SO_4^{2-} anions], 440 ($Fe^{3+}\cdots$O stretching vibrations and/or $\nu_2(E)$ bending mode of SO_4^{2-} anions).

The IR spectrum of magnesiovoltaite is similar to that of voltaite (Fig. 4b), but in the former most absorption bands are shifted towards higher frequencies since the atomic mass of magnesium is less than that of iron. The IR spectrum of the tetragonal voltaite-group mineral pertlikite (Fig. 4c) differs from those of voltaite and magnesiovoltaite in additional, poorly resolved splitting of some bands.

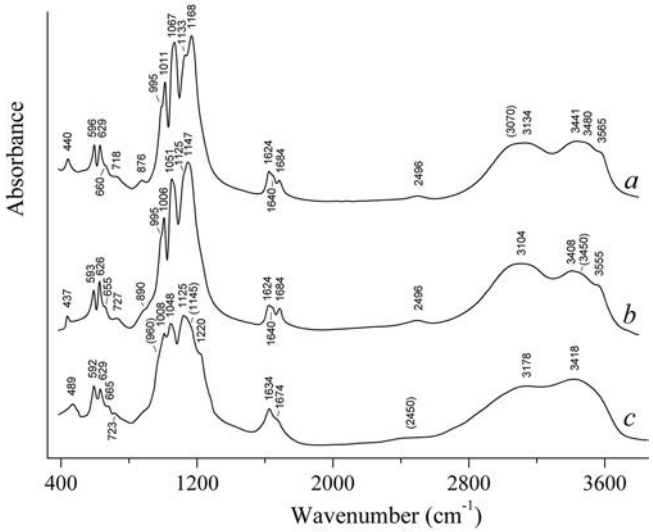

Fig. 4. The IR spectra of (*a*) magnesiovoltaite, (*b*) black voltaite with Fe^{2+}:Mg ≈ 6:1 from the Alcaparrosa mine, and (*c*) dark olive green pertlikite from La Fossa crater, Vulcano island, Sicily, Italy.

The line broadening may be caused by different configurations of Fe-centred octahedra, variations of their local environments, as well as by chemical heterogeneity of the mineral.

The distribution of the hyperfine parameters has been restored using the software SpectrRelax (Matsnev & Rusakov, 2012; see Fig. 6). The reconstruction of the distribution was carried out under the assumption of linear correlation between the isomer shift (*IS*) and quadrupole splitting (*QS*). Table 1 shows parameters of the isomer shift and quadrupole splitting distribution for the Mössbauer spectrum of magnesiovoltaite: the maximum (*max*) and average (*aver*) values of the isomer shift and quadrupole splitting, as well as the linear correlation coefficient for them ($\Delta IS/\Delta QS$).

Unlike magnesiovoltaite, voltaite shows a room-temperature Mössbauer spectrum containing an additional strong doublet with *IS* ~ 1.2 – 1.3 and *QS* ~ 1.6 – 1.8 mm/s corresponding to Fe^{2+} in octahedral coordination (Long *et al.*, 1980; Ertl *et al.*, 2008; Majzlan *et al.*, 2013).

Mössbauer spectroscopy

The ^{57}Fe Mössbauer spectrum was collected in constant-acceleration transmission mode, in the velocity range ±4 mm s^{-1}, with a 10 mCi ^{57}Co/Rh source, at 298 K. Data were stored in a 1024-channel MCS memory unit. Isomer shifts were calculated relative to α-Fe.

The Mössbauer spectrum of magnesiovoltaite (Fig. 5) can be approximated by one symmetric pseudo-Voigt doublet with the following parameters corresponding to Fe^{3+} in octahedral oxygen coordination:

- Isomer shift 0.360(4) mm/s;
- Quadrupole splitting 0.32(1) mm/s;
- Line width 0.55 (3) mm/s.

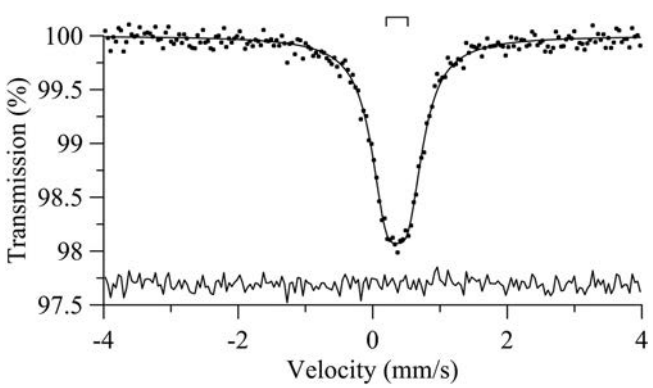

Fig. 5. The ^{57}Fe Mössbauer spectrum of magnesiovoltaite and its fitting by one pseudo-Voigt quadrupole doublet.

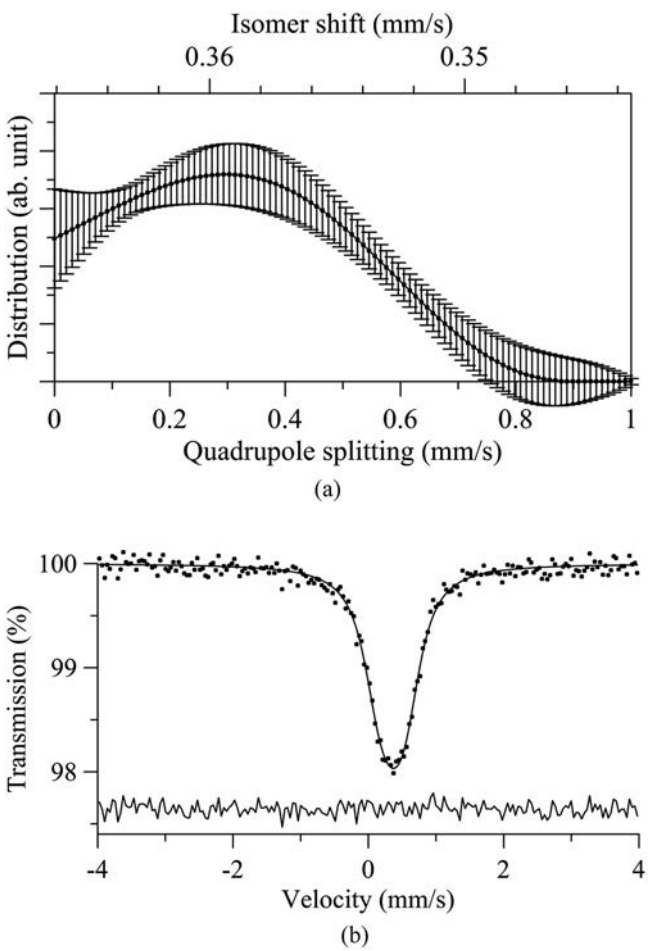

Fig. 6. The result of the restoration of hyperfine parameters distribution (a) and the ^{57}Fe Mössbauer spectrum of magnesiovoltaite with its fitting based on this distribution (b).

Table 1. Parameters of the isomer shift and quadrupole splitting distribution for the Mössbauer spectrum of magnesiovoltaite.

IS_{max}, mm/s	QS_{max}, mm/s	IS_{aver}, mm/s	QS_{aver}, mm/s	$\Delta IS/\Delta QS$
0.360(11)	0.29(8)	0.359(4)	0.324(24)	–0.022(35)

Chemical data

Five chemical analyses were carried out using an electron microprobe (EDS mode, 20 kV, 600 pA, beam rastered over the area 16 × 16 μm) with a digital scanning electron microscope Tescan VEGA-II XMU equipped by an energy-dispersive spectrometer INCA Energy 450. H_2O was determined by gas chromatography of products of the mineral ignition at 1200 °C with a Vario Micro cubeanalyser (Elementar GmbH, Germany). CO_2 was not analysed because of the absence of absorption bands corresponding to vibrations of C–O bonds in the IR spectrum. Analytical data are given in Table 2. Contents of other elements with atomic number higher than 8 are below detection limits.

The empirical formula (based on 66 O *apfu*) is $(K_{1.85}Na_{0.08})(Mg_{4.25}Mn_{0.46}Zn_{0.14})Fe^{3+}{}_{3.14}Al_{0.91}(SO_4)_{11.91}(H_2O)_{18.325}O_{0.035}$.

In the investigated crystal, peripheral parts are enriched in Mg as compared to core. The contents of MgO and Fe_2O_3 are, respectively (wt.%): 8.52-8.55 and 13.60-13.68 (in the core of the crystal), 9.13 and 13.51 (in the intermediate zone); 9.72-9.73 and 12.96-13.05 (in the peripheral part of the crystal).

The simplified formula is $K_2Mg_5Fe^{3+}{}_3Al(SO_4)_{12}\cdot 18H_2O$.

The Gladstone-Dale compatibility index is: $1 - (K_p/K_c) = -0.013$ ("superior").

Sensitive tests with potassium hexacyanoferrate(II) and potassium hexacyanoferrate(III) show that all iron is trivalent in magnesiovoltaite from the botryogen-bearing assemblage. In magnesiovoltaite associated with coquimbite almost all iron is trivalent, but traces of Fe^{2+} are also present.

X-ray diffraction (XRD) data and crystal structure

The powder XRD pattern of magnesiovoltaite (Table 3) was obtained using a Rigaku R-AXIS Rapid II diffractometer with curved image plate (d = 127.4 mm, Debye-Scherrer geometry, Co$K\alpha$, 40 kV, 15 mA, 12 min exposure). The a parameter of the cubic unit cell refined from powder data is equal to 27.17(1) Å; V = 20057(20) Å^3.

The single-crystal X-ray diffraction data were collected at room temperature by means of a SMART APEX2 diffractometer (*APEX*2 2009) with graphite monochromatized Mo$K\alpha$ radiation (λ = 0.71073 Å) and a CCD detector using the ω–θ scanning mode. Raw data were integrated using the program SAINT and scaled, merged, and corrected for Lorentz-polarization effects using the SADABS package. A total of 62555 reflections within the sphere limited by θ = 30.62° were measured. The experimental details of the data collection and refinement results are listed in Table 4. The structure refinement was carried out using the JANA2006 program package (Petříček *et al*., 2006). Illustrations were produced with the JANA2006 program package in combination with the DIAMOND program (Brandenburg & Putz, 2005).

The symmetry of minerals with voltaite-type structure as well as their synthetic analogues is cubic (space group $Fd\bar{3}c$), but different kinds of cation ordering lead to symmetry lowering from cubic to tetragonal with formation of the pertlikite-type structure (space group $I4_1/acd$). The "traditional" space group $Fd\bar{3}c$ (with the origin at $\bar{3}$) corresponding to the voltaite-type structure was chosen for magnesiovoltaite based on the analysis of systematic absences of reflections. Atomic scattering factors for neutral atoms together with anomalous dispersion

Table 2. Chemical composition (wt.%) of magnesiovoltaite.

Constituent	Mean	Range	Standard deviation	Probe standard
Na_2O	0.13	0 – 0.25	0.07	Albite
K_2O	4.64	4.43 – 4.77	0.13	Orthoclase
MgO	9.13	8.52 – 9.73	0.45	Diopside
MnO	1.73	1.64 – 1.94	0.12	$MnTiO_3$
ZnO	0.84	0.53 – 1.22	0.22	Zn
Al_2O_3	2.47	2.23 – 2.84	0.21	Albite
Fe_2O_3*	13.36	12.96 – 13.68	0.30	Fe_2O_3
SO_3	50.83	50.34 – 51.38	0.46	$BaSO_4$
H_2O	17.6±0.5			
Total	100.73			

*In accordance with Mössbauer data all iron is considered as Fe^{3+}.

Table 3. Powder X-ray diffraction data for magnesiovoltaite.

I_{obs}, %	d_{obs}, Å	I_{calc}, %*	d_{calc}, Å**	h	k	l
29	9.56	76	9.60	0	2	2
14	7.82	12	7.84	2	2	2
37	6.77	2	6.79	0	0	4
61	5.53	100	5.54	2	2	4
2	4.79	3	4.80	0	4	4
10	4.58	7	4.59	1	3	5
6	4.28	6	4.295	0	2	6
8	4.09	5	4.095	2	2	6
13	3.915	10	3.920	4	4	4
17	3.626	6	3.630	2	4	6
68	3.532	28	3.536	1	3	7
100	3.392	40	3.395	0	0	8
12	3.199	10	3.201	2	2	8
22	3.133	8	3.136	1	5	7
45	3.034	39	3.037	0	4	8
11	2.979	6	2.981	3	5	7
5	2.893	4	2.895	4	6	6
30	2.845	13	2.847	1	3	9
7	2.768	2	2.772	4	4	8
2	2.662	5	2.663	0	2	10
11	2.618	4	2.626	1	5	9
		1	2.614	2	2	10
		2	2.614	6	6	6
24	2.531	12	2.533	3	5	9
		2	2.522	4	6	8
8	2.400	3	2.401	0	8	8
6	2.363	1	2.364	4	4	10
		2	2.364	2	8	8
1	2.328	1	2.329	0	6	10
10	2.263	10	2.263	0	0	12
		2	2.263	4	8	8
1	2.202	5	2.203	2	2	12
10	2.181	2	2.182	3	5	11
		2	2.182	5	7	9
3	2.120	1	2.121	2	4	12
		1	2.121	6	8	8
23	2.076	13	2.077	1	7	11
		1	2.071	6	6	10
3	2.047	4	2.047	4	4	12
3	2.027	1	2.025	4	8	10
4	2.002	1	2.002	2	6	12
1	1.960	1	1.960	8	8	8
5	1.902	3	1.902	2	2	14
5	1.883	3	1.883	0	8	12
4	1.865	1	1.866	2	8	12
		1	1.848	2	4	14
5	1.815	6	1.815	4	8	12
3	1.803	2	1.803	3	7	13
6	1.772	2	1.772	1	3	15
3	1.725	1	1.725	4	6	14
		2	1.725	2	10	12
5	1.715	1	1.714	1	9	13
		1	1.714	7	9	11
2	1.698	1	1.698	0	0	16
		1	1.688	3	9	13
1	1.685	1	1.685	4	10	12
5	1.672	3	1.672	2	8	14
		1	1.672	8	10	10
3	1.659	2	1.659	6	6	14
1	1.647	2	1.647	0	4	16
2	1.623	2	1.623	6	10	12
		1	1.615	3	7	15
11	1.601	8	1.601	4	4	16
		1	1.601	0	12	12
3	1.590	2	1.590	2	12	12
		1	1.579	0	10	14
8	1.571	3	1.571	1	3	17
		1	1.571	5	7	15
		1	1.571	3	11	13
		2	1.568	2	10	14
2	1.558	1	1.558	4	12	12
2	1.548	1	1.548	8	10	12
5	1.531	2	1.530	1	5	17
		1	1.530	3	9	15
1	1.519	2	1.518	0	8	16
2	1.510	1	1.509	8	8	14
2	1.482	1	1.482	4	8	16
3	1.448	3	1.448	8	12	12
2	1.441	1	1.442	3	11	15
		1	1.440	6	8	16
2	1.432	1	1.432	0	6	18
5	1.426	3	1.426	5	7	17
1	1.411	1	1.410	5	11	15
3	1.402	1	1.401	4	6	18
		1	1.401	6	12	14
		1	1.372	6	10	16
4	1.367	2	1.367	1	13	15
1	1.359	1	1.358	0	12	16

(*continued*)

*For the calculated pattern, only reflections with intensities ≥1 are given.
**For the unit-cell parameter calculated from single-crystal data.

corrections were taken from *International Tables for X-Ray Crystallography* (Ibers & Hamilton, 1974). The initial model for the magnesiovoltaite structure refinement was based on the atom coordinates for synthetic "Fe20Mg80-voltaite" (Majzlan *et al.*, 2013).

The final refinement cycles converged to R_1 = 3.21, wR_2 = 5.37, and GooF = 1.01 for 1147 independent reflections with $I > 2\sigma(I)$. The highest peak and the deepest hole in the final residual electron density map are 0.88 and −0.37 e Å^{-3}, respectively. Table 5 shows the fractional atomic coordinates, occupancy, site symmetry and equivalent atomic displacement parameters. Anisotropic atomic displacement parameters are presented in Table 6. Table 7 reports selected interatomic distances. Bond-valence sum calculations (Table 8) were performed using the bond-length parameters from Brown & Altermatt (1985).

The voltaite-type structure is very complex and can be obtained by an assemblage of fundamental building units (FBUs). These FBUs are heteropolyhedral clusters with the general formula $\{M_8[TX_4]_{12}\varphi_8\}$ formed by isolated MO$_6$-octahedra linked *via* $[TX_4]$-tetrahedra (Fig. 7a,b). The detailed crystal-chemical formula of FBU in the case of voltaite-type structures ($T = S^{6+}$; $X = O^{2-}$ and $\varphi = H_2O$) can be written as follows: $\{[M(1)(H_2O)_2]_4M(2)_4[SO_4]_{12}\}$, where M are di- and trivalent cations Mg^{2+}, Al^{3+}, Fe^{2+}, Fe^{3+}, Mn^{2+}, Zn^{2+}, Cd^{2+}. Adjacent FBUs are polymerized into heteropolyhedral columns (Hawthorne *et al.*, 2000) stretching along *x, y* and *z* axes. The columns form a

Table 4. Crystal parameters, data collection and structure refinement details for the crystal of magnesiovoltaite.

Crystal data	
Formula	$K_2Mg_5Fe_3Al(SO_4)_{12}\cdot 18H_2O$
Formula weight (g)	1859.8
Temperature (K)	293
Cell setting	Cubic
Space group	$Fd\bar{3}c$
a (Å)	27.161(1)
V (Å^3)	20038(2)
Z	16
Crystal size (mm)	0.13×0.13×0.17
Crystal form	Anhedral grain
Data collection	
Diffractometer	Bruker SMART APEX2 CCD
Radiation; λ	Mo$K\alpha$; 0.71073
Absorption coefficient, μ (mm^{-1})	1.996
F (000)	14715
Data range θ (º); h, k, l	2.12–30.62; $-38<h<38, -38<k<38, -38<l<38$
No. of measured reflections	62555
Total reflections (N_2)/observed(N_1)	1278/1147
Criterion for observed reflections	$I > 2\sigma(I)$
R_{int} (%)	7.17
Refinement	
Refinement on	Full-matrix least squares on F
Weight scheme	$1/(\sigma^2\|F\|+ 001936\ F^2)$
R_1, wR_2	3.21, 5.37
GooF (Goodness of fit)	1.01
Max./min. residual e density (eÅ^{-3})	0.88 /–0.37

Note: $R_1 = \sum||F_{obs}|-|F_{calc}||/\sum|F_{obs}|$; $wR_2 = \{\sum[w(F_{obs}^2 - F_{calc}^2)^2] / \sum[w(F_{obs}^2)^2]\}^{1/2}$;
GooF = $\{\sum[w(F_{obs}^2 - F_{calc}^2)] /(n-p)\}^{1/2}$ where n is the number of reflections and p is the number of refined parameters.

Table 5. Fractional site coordinates, site multiplicities (Q), equivalent displacement parameters of atoms (U_{eq}, Å^2) and site composition in the structure of magnesiovoltaite.

Site	x	y	z	Q	U_{eq}	population
K	0.25	0.25	0.25	32b	0.0283(2)	$K_{0.95}Na_{0.05}$
$M1$	0.25	0.1029(1)	-0.1029(1)	96g	0.0103(1)	$Mg_{0.71}(Fe^{3+},Mn,Zn)_{0.29}$
$M2$	0	0	0	32c	0.0109(1)	$Fe^{3+}_{1.00}$
Al	0.125	0.125	0.125	16a	0.0133(2)	$Al_{0.9}Fe^{3+}_{0.1}$
S	0.2379(1)	0.2756(1)	0.1186(1)	192h	0.0102(1)	S
O1	0.2497(1)	0.2467(1)	0.0737(1)	192h	0.0175(4)	O
O2	0.2258(1)	0.3265(1)	0.1049(1)	192h	0.0207(4)	O
O3	0.1949(1)	0.2545(1)	0.1432(1)	192h	0.0264(5)	O
O4	0.2805(1)	0.2743(1)	0.1519(1)	192h	0.0216(4)	O
Ow5	0.3191(1)	0.0786(1)	-0.1215(1)	192h	0.0235(4)	H_2O
Ow6	0.1791(2)	0.1603(2)	0.1469(2)	192h	0.023(2)	$\square_{0.75}(H_2O)_{0.25}$
Ow7	0.1802(2)	0.1607(3)	0.1029(2)	192h	0.025(2)	$\square_{0.75}(H_2O)_{0.25}$

Note: U_{eq} is defined as one third of the trace of the orthogonalized U_{ij} tensor.

heteropolyhedral framework (Fig. 8) with large cavities having $\{4^{24}8^{6}12^{4}\}$ topology. In voltaite and magnesiovoltaite these cavities are occupied by disordered AlO_6-octahedra (Fig. 9a,b). The microporous voltaite-type structure is characterized by a three-dimensional system of channels with eight-membered cross-section which are parallel to the heteropolyhedral columns and pass through the centres of the cavities. The alkaline A^+-ions are arranged at twelve-membered windows between adjacent cavities (Fig. 9c).

Magnesiovoltaite is isostructural with other cubic voltaite-group minerals, namely voltaite (Mereiter, 1972), zincovoltaite (Wanmao *et al*., 1987) and ammoniomagnesiovoltaite (Szakáll *et al*., 2012) – see Figs. 9 and 10, as well as their synthetic analogues (Majzlan *et al*., 2013). Based on the refined site-scattering factors, the crystal-chemical formula

Table 6. Anisotropic atomic displacement parameters (Å^2) for magnesiovoltaite.

Site	U^{11}	U^{22}	U^{33}	U^{12}	U^{13}	U^{23}
K	0.0283(3)	0.0283(3)	0.0283(3)	0.0126(3)	0.0126(3)	0.0126(3)
*M*1	0.0112(3)	0.0099(2)	0.0099(2)	-0.0005(1)	-0.0005(1)	-0.0009(2)
*M*2	0.0109(2)	0.0109(2)	0.0109(2)	0.0023(1)	0.0023(1)	0.0023(1)
Al	0.0133(4)	0.0133(4)	0.0133(4)	0	0	0
S	0.0102(2)	0.0100(2)	0.0104(2)	-0.0003(1)	-0.0002(1)	-0.0004(1)
O1	0.0215(7)	0.0182(6)	0.0129(7)	0.0040(5)	-0.0027(5)	-0.0038(5)
O2	0.0303(8)	0.0110(6)	0.0209(7)	0.0009(5)	-0.0020(6)	0.0009(5)
O3	0.0212(8)	0.0250(7)	0.0332(9)	-0.0074(6)	0.0116(6)	-0.0006(6)
O4	0.0170(6)	0.0350(8)	0.0128(6)	0.0058(5)	-0.0035(5)	-0.0064(5)
Ow5	0.0167(6)	0.0320(8)	0.0217(7)	0.0056(6)	0.0025(5)	-0.0001(6)
Ow6	0.019(3)	0.019(3)	0.031(3)	0.001(2)	-0.010(2)	0.002(2)
Ow7	0.016(3)	0.027(3)	0.033(3)	-0.003(2)	0.002(2)	-0.003(3)

Table 7. Selected interatomic distances and O–S–O angles in magnesiovoltaite.

Bond		Bond length, Å	Bond		Bond length, Å
K–	O4	2.867(1) x6	Al–	Ow6	1.853(5) x3
	O3	3.267(2) x6		Ow7	1.884(6) x3
mean		3.067	mean		1.869
*M*1–	O2	2.027(2) x2	S–	O3	1.464(2)
	Ow5	2.053(2) x2		O2	1.468(2)
	O4	2.079(2) x2		O4	1.470(1)
mean		2.053		O1	1.485(2)
BLDP$^{(M1)}$		0.011	mean		1.472
ELDP$^{(M1)}$		20.09	Angle		Angle value, °
*M*2–	O1	2.004(2) x6	O1–S–O2		109.92(8)
mean		2.004	O1–S–O3		109.81(9)
BLDP$^{(M2)}$		0	O1–S–O4		108.82(8)
ELDP$^{(M2)}$		25.37	O2–S–O3		107.85(9)
			O2–S–O4		110.75(9)
			O3–S–O4		109.68(9)

Note: In accordance with Majzlan *et al.* (2013), bond-length distortion parameters (BLDP) and edge-length distortion parameters (ELDP) are defined as follows (Griffen & Ribbe, 1979):

$$\mathrm{BLDP} = \frac{1}{\langle Cat\text{–}\mathrm{O}\rangle}\left\{\frac{\sum_{i=1}^{x}\left[(Cat\text{–}\mathrm{O})_i - \langle Cat\text{–}\mathrm{O}\rangle\right]^2}{x-1}\right\}^{\frac{1}{2}}, \mathrm{ELDP} = \frac{1}{\langle \mathrm{O}\text{–}\mathrm{O}\rangle}\left\{\frac{\sum_{i=1}^{y}\left[(\mathrm{O}\text{–}\mathrm{O})_i - \langle \mathrm{O}\text{–}\mathrm{O}\rangle\right]^2}{y-1}\right\}^{\frac{1}{2}} \times 1000,$$

where x = 4 and y = 6 for tetrahedra (with 4 cation – anion (*Cat*–O) and 6 anion – anion (O–O) distances, respectively); x = 6 and y = 12 for octahedra (with 6 (*Cat*–O) and 15 (O–O) distances, respectively).

Table 8. Bond valence calculations for magnesiovoltaite.

Site	O1	O2	O3	O4	Ow5	Ow6	Ow7	∑cation
K			$0.04^{\times 6\rightarrow}$	$0.13^{\times 6\rightarrow}$				1.02
			$0.04^{\downarrow}$	$0.13^{\downarrow}$				
*M*1		$0.42^{\times 2\rightarrow}$		$0.37^{\times 2\rightarrow}$	$0.39^{\times 2\rightarrow}$			2.36
		$0.42^{\downarrow}$		$0.37^{\downarrow}$	$0.39^{\downarrow}$			
*M*2	$0.52^{\times 6\rightarrow}$							3.12
	$0.52^{\downarrow}$							
Al						$0.56^{\times 3\rightarrow}$	$0.51^{\times 3\rightarrow}$	3.21
						$0.56^{\downarrow}$	$0.51^{\downarrow}$	
S	1.54	1.61	1.63	1.60				6.38
∑anion	2.06	2.03	1.67*	2.10	0.39	0.42**	0.38**	

*Non-bridging oxygen atom: O3 is an acceptor for hydrogen atoms of Ow5-donor oxygen ($D^{\mathrm{Ow5}}\cdots A^{\mathrm{O3}}$ = 2.89 Å) and partly occupied Ow6- and Ow7-oxygens ($D^{\mathrm{Ow6}}\cdots A^{\mathrm{O3}}$ = 2.47 Å or 2.60 Å; $D^{\mathrm{Ow7}}\cdots A^{\mathrm{O3}}$ = 2.80 Å or 2.81 Å).
**BVS is obtained by multiplying on site occupancy factor (taking into account site multiplicity).
Note: In mixed sites, bond-valence contribution of each cation has been weighted according to its occupancy.

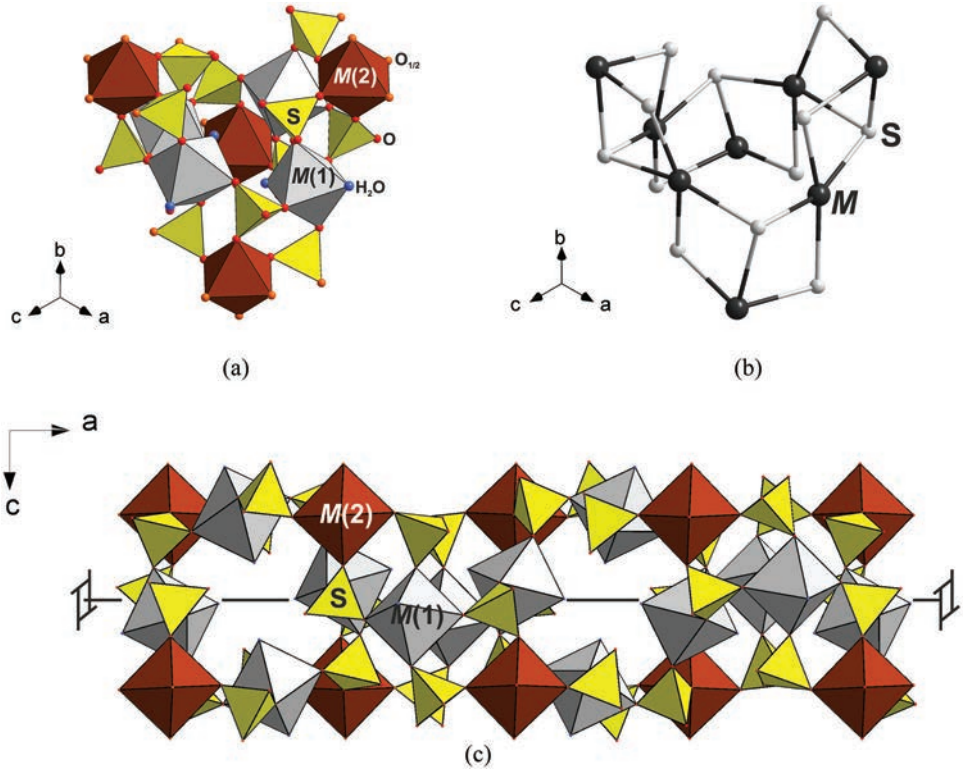

Fig. 7. Fundamental building unit represented by heteropolyhedral cluster in the voltaite-type structures [general view (a) and graph representation (b)] and heteropolyhedral column formed by condensation of clusters which are rotated by the 4_1-axes (c). For legend see Table 5. (online version in colour)

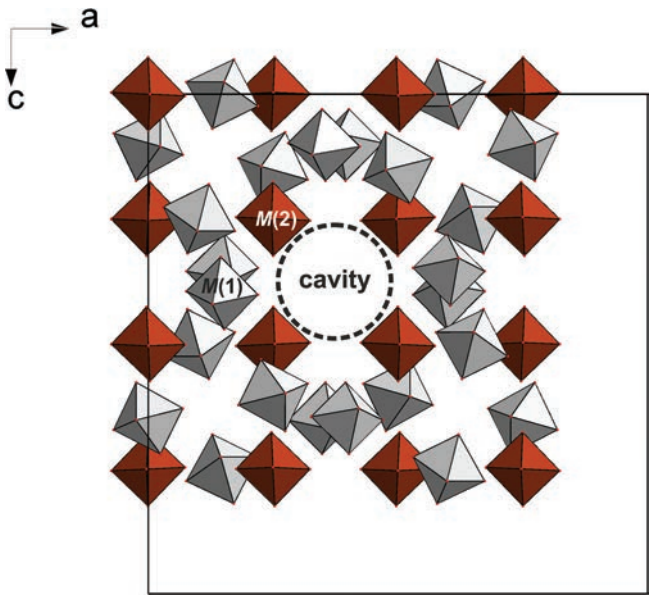

Fig. 8. Crossing of the heteropolyhedral column by the channel with formation of the cavity. SO_4-tetrahedra are omitted, the unit cell is outlined. (online version in colour)

of magnesiovoltaite can be written as follows (Z = 16): $^{A}(K_{1.9}Na_{0.1})[(Al_{0.9}Fe^{3+}_{0.1})(H_2O)_6]$ $^{M(1)}\{Mg_{4.3}(Fe^{3+},Mn,Zn)_{1.7}(H_2O)_{12}$ $^{M(2)}Fe^{3+}_{2}$ $(SO_4)_{12}\}$, where the composition of the heteropolyhedral framework is put in figure brackets. The idealized crystal-chemical formula of magnesiovoltaite, according to recommendations of the International Zeolite Association (Liebau, 2003; McCusker, 2005), can be written as follows (Z = 16):

$$|K_2^{[12]}\ Al^{[6]}\ (H_2O)_6|[(Mg_5Fe_3^{3+})^{[6]}\ (SO_4)_{12}\ (H_2O)_{12}]_h\{3\}_p\ \{0[4^{24}8^6 12^4]/3[100](8\text{-ring})\}(Fd\bar{3}m),$$

indicating that (i) the guests are K^+ ions and the $[Al(H_2O)_6]^{3+}$ complex and (ii) the 3D host structure consists of cavities as well as a three-dimensional channel system with an eight-membered ring pore opening along the [100] direction.

Discussion

Although sulfur is only the fifteenth most abundant element in the continental crust of the Earth (Hawthorne *et al.*, 2000), sulfates are one of the largest classes of minerals. However, their diversity is associated mainly with a few types of parageneses. Of about 600 new mineral species discovered during five years (in the period 2011 – 2015), 84 minerals (*i.e.* every seventh species) contain SO_4^{2-} group; 45 of them (including eleven minerals, mainly uranium ones, from Blue Lizard Mine, Utah, USA, six uranium sulfates from the Jáchymov ore district, Czech Republic, and seven sulfates from arid areas of northern Chile) are related to the oxidation zone of ore

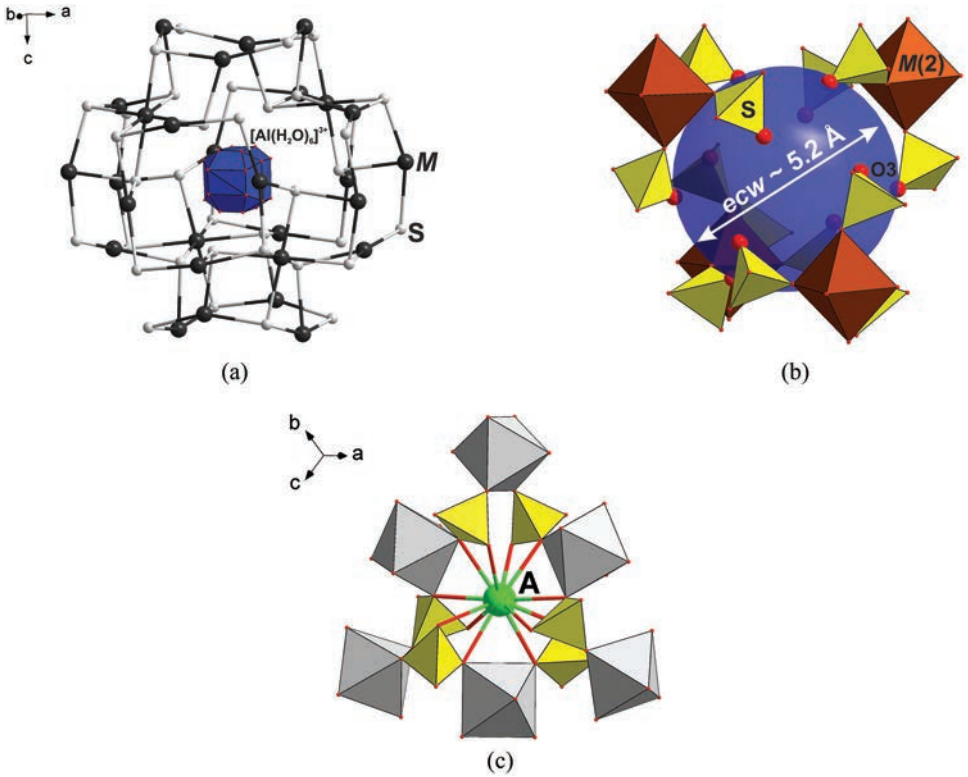

Fig. 9. Large cavity with $\{4^{24}8^{6}12^{4}\}$-topology occupied by the distorted octahedral complex $Al(H_2O)_6$ (a), effective cavity width (McCusker, 2005) delimited by O3-oxygen atoms (b) and twelve-membered window of cavity occupied by a monovalent A-cation (c) in the voltaite-type structure. (online version in colour)

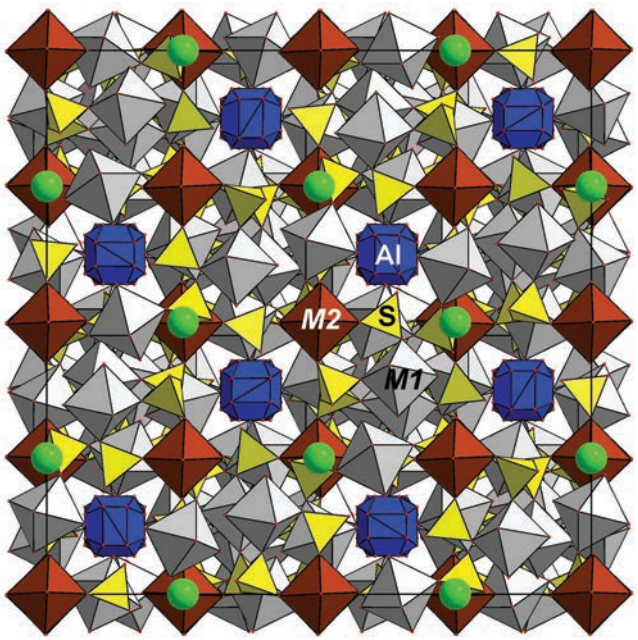

Fig. 10. The crystal structure of magnesiovoltaite: general view; the unit cell is outlined. The spheres correspond to K cations. (online version in colour)

deposits, and 30 sulfate minerals (including 20 species from the Tolbachik volcano, Kamchatka peninsula, Russia and nine species from the La Fossa crater, Vulcano Island, Italy) are products of volcanic exhalations or condensation of gases in oil-shale fires.

Only nine minerals discovered in the period 2011 – 2015 and containing SO_4^{2-} group are related to other types of geological formations and are products of pyrometamorphism, metasomatism, hydrothermal processes, *etc*. All of them, except kottenheimite, contain additional oxyanions SiO_4^{4-}, SO_3^{2-}, CO_3^{4-}, $B(OH)_4^{-}$, $B_5O_8(OH)^{2-}$, or PO_4^{3-}.

It is noteworthy that in recent years the proportion of sulfates among the newly discovered minerals increases. Among new minerals approved in 2015 by the IMA Commission on New Minerals, Nomenclature and Classification, every fourth mineral contains SO_4^{2-} group.

The sulfate minerals discovered recently in arid areas of northern Chile are alcaparrosaite $K_3TiFe^{3+}(SO_4)_4O{\cdot}2H_2O$ (Kampf *et al*., 2012), witzkeite $Na_4K_4Ca(NO_3)_2(SO_4)_4{\cdot}2H_2O$ (Nestola *et al*., 2012), vendidaite $Al_2(SO_4)(OH)_3Cl{\cdot}6H_2O$ (Chukanov *et al*., 2013), camaronesite $Fe^{3+}{}_2(HPO_4)_2(SO_4){\cdot}5–6H_2O$ (Kampf *et al*., 2013), möhnite $(NH_4)K_2Na(SO_4)_2$ (Chukanov *et al*., 2015), riotintoite $Al(SO_4)(OH){\cdot}3H_2O$ (Chukanov *et al*., 2016), and magnesiovoltaite (this work). However the mineralogy of the oxidation zone of ore deposits of northern Chile has been insufficiently studied. Most of these deposits are located in the area of arid climate, and in most cases secondary sulfate minerals were formed under highly acidic conditions.

Magnesiovoltaite is a member of the voltaite group (see Table 9). It is the Mg-dominant analogue of voltaite

Table 9. Comparative data for voltaite-group minerals.

Mineral	Magnesio-voltaite	Voltaite	Zincovoltaite	Ammonio-magnesiovoltaite	Pertlikite
Simplified formula	$K_2Mg_5Fe^{3+}{}_3Al(SO_4)_{12}\cdot 18H_2O$	$K_2Fe^{2+}{}_5Fe^{3+}{}_3Al(SO_4)_{12}\cdot 18H_2O$	$K_2Zn_5Fe^{3+}{}_3Al(SO_4)_{12}\cdot 18H_2O$	$(NH_4)_2Mg_5Fe^{3+}{}_3Al(SO_4)_{12}\cdot 18H_2O$	$K_2(Fe^{2+},Mg)_2(Mg,Fe^{3+})_4Fe^{3+}{}_2Al(SO_4)_{12}\cdot 18H_2O$
Crystal system	Cubic	Cubic	Cubic	Cubic	Tetragonal
Space group	*Fd–3c*	*Fd–3c*	*Fd–3c*	*Fd–3c*	$I4_1/acd$
a, Å	27.161	27.254	27.180	27.260	19.2080
c, Å					27.2158
V, Å^3	20038	20244	20079	20257	10041.2
Z	16	16	16	16	8
Strong lines of the powder X-ray diffraction pattern: *d*, Å (*I*, %)	9.56 (29) 6.77 (37) 5.53 (61) 3.532 (68) 3.392 (100) 3.034 (45) 2.845 (30)	9.66 (30) 6.79 (30) 5.57 (70) 3.54 (100) 3.41 (90) 3.15 (30) 3.04 (50)	5.53 (48) 4.24 (28) 3.84 (32) 3.54 (67) 3.39 (100) 3.13 (39) 3.03 (28)	6.85 (24) 5.59 (100) 3.562 (66) 3.420 (72) 1.7836 (25) 1.5582 (25)	5.543(28) 3.396(100) 3.136(21) 3.038(39) 2.848(31) 2.534(21) 2.078(29) 1.601(21)
Colour (megascopic)	Yellow to yellowish-greenish	Dark green to black	Dark green (Fe^{2+}-bearing variety)	Yellow to brown	Dark green to black
Optical data	Anomalously uniaxial or biaxial (–); n_{min} = 1.584, n_{max} = 1.588	Anomalously biaxial (–); n_{min} = 1.593, n_{max} = 1.608	Isotropic or anomalously uniaxial; $n_{mean} \approx 1.605$	Isotropic; n = 1.60	Uniaxial (–); ω = 1.590, ε = 1.586
Density, g·cm^{-3}	2.51 (meas.) 2.506 (calc.)	2.645 (meas.) 2.663 (calc.)	2.765 (meas.) 2.767 (calc.)	2.55 (meas.) 2.351 (calc.)	2.59 (meas.) 2.56 (calc.)
Sources	This work	Mereiter, 1972; Sakurai *et al.*, 1958	Wanmao *et al.*, 1987	Szakáll *et al.*, 2012	Ertl *et al.*, 2008

and zincovoltaite (Mg > Fe^{2+}, Zn) and the K-dominant (K > NH_4) analogue of ammoniomagnesiovoltaite.

Although magnesiovoltaite is rare in comparison to voltaite, Mg-dominant voltaite-group minerals have been described in several localities. One of the analyses included for voltaite by Palache *et al*. (1951) corresponds to magnesiovoltaite. An Mg-dominant analogue of voltaite was described in a sulfate association precipitated around a geyser located in the Western Cordillera of southern Peru (Ciesielczuk *et al*., 2013), but chemical analysis of this mineral is not given in the cited paper. Mg-dominant sites are present in the structures of ammoniomagnesiovoltaite and pertlikite. Voltaite from a weathered massive sulfide deposit at Iron Mountain, California contains from 0.53 to 1.17 *apfu* Mg (Majzlan *et al*., 2011). When crystallizing under oxidizing conditions, occurrence of Mg in the *M*1 site may be due to deficiency of Fe^{2+} in the mineral-forming solution. In the Alcaparrosa mine massive andesitic and dacitic host rocks are the possible source of Mg for magnesiovoltaite, pickeringite and magnesiocopiapite.

Based on numerous observations, it was concluded (Jambor *et al*., 2000) that the following transformation (oxidation) sequence is typical for sulfide deposits in arid conditions: iron sulfides → melanterite → siderotil + szomolnokite + copiapite → rhomboclase + römerite + voltaite + bilinite. However, our observations show a somewhat different sequence of mineral formation in the Alcaparrosa mine: pyrite → szomolnokite + rhomboclase → römerite + metavoltine + voltaite → coquimbite → magnesiovoltaite. Only two sulfates, szomolnokite and rhomboclase, were observed in direct contact with pyrite, but rhomboclase is present also in later sulfate associations.

Association with rhomboclase is typical for voltaite, which indicates highly acidic conditions of crystallization (Jambor *et al*., 2000). In this respect it is appropriate to note that synthetic Fe^{2+}-bearing magnesiovoltaite was obtained as black octahedral crystals in late stages of evaporation of a solution containing sulfates of K, Na, Fe^{2+}, Fe^{2+}, Mg, Ca and Al, as well as H_2SO_4 and HCl, at initial pH of 2.0 (Tosca & McLennan, 2009). During evaporation, the brine evolved to a highly acidic (pH –1.3) solution depleted in Ca, Al and K. Other sulfates formed together with magnesiovoltaite in this experiment are rhomboclase, gypsum and Fe^{2+}-bearing magnesium sulfate.

The light yellow to pale green colour is an important diagnostic feature of Fe^{2+}-poor magnesiovoltaite. As noted by Majzlan *et al*. (2013), synthetic voltaite analogues with any amount of Fe^{2+} are macroscopically black and dark green in thin sections, whereas voltaite-type compounds in which Fe^{2+} is completely replaced by Zn, Mg, or Cd are yellow. Synthetic magnesiovoltaite containing 0.58 apfu Fe^{2+} is black (Tosca & McLennan, 2009).

Most voltaite and zincovoltaite samples (see Table 7), as well as structurally studied synthetic analogues of voltaite, magnesiovoltaite and zincovoltaite, which have cubic symmetry, are also optically anisotropic, although chemical profiles showed no hints of elemental variations that could explain the optical anomalies (Majzlan *et al*., 2013). The anomalous anisotropy of cubic crystals may be explained by their deformation caused by the stress due to different degree of dehydration in different zones or sectors. An additional possible cause of the anisotropy is deformation of the crystals during their growth or when they were crushed.

The anisotropy caused by deformation is well known for a number of materials including even X-ray amorphous glass. The optical anisotropy is known for many other minerals of the cubic crystal system (diamond, analcime, garnets, spinel-group members, pharmacosiderite, nabiasite, *etc*.) and is described in numerous publications (*e.g*. Buerger *et al*., 1967; Howell, 2012; Shtukenberg & Punin, 2007; Hariya & Kimura, 1978; Allen & Buseck, 1988; McAloon & Hofmeister, 1993; Antao *et al*., 2014; Libowitzky, 1994; Akizuki, 1981; Brugger *et al*., 1999). Such crystals are often called "optically anomalous crystals". The causes of optical anomalies are discussed in detail by Shtukenberg & Punin (2007).

Acknowledgements

The authors are grateful to G. Giester and an anonymous reviewer for valuable comments. For the mineralogical investigations and determination of chemical composition, physical properties and powder X-ray diffraction data, this work was financially supported by the Russian Foundation for Basic Research (grant no. 14-05-00190-a) as well as grants FAPEMIG (APQ-01448-15), PROPP/UFOP (2/2015) and CNPq (305284/2015-0). S.M.A is grateful for financial support of the Russian Foundation for Basic Research (grant no. 16-35-60101) for the crystal structure refinement. The technical support by the SPbSU X-Ray Diffraction Research Resource Center in the XRD powder-diffraction studies is acknowledged.

References

APEX2 (2009): Bruker AXS Inc. USA, Madison, Wisconsin.

Akizuki, M. (1981): Origin of optical variation in analcime. *Am. Mineral.*, **66**, 403–409.

Allen, F.M. & Buseck, P.R. (1988): XRD, FTIR, and TEM studies of optically anisotropic grossular garnets. *Am. Mineral.*, **73**, 568–584.

Antao, S.M., Zaman, M.M., Klinker, A.M., Round, S., Gontijo, V.L., Camargo, E.S. (2014): Garnet: intergrowths, multi-phases, and optical anisotropy. Papers of the 2014th GSA Annual Meeting. Vancouver, British Columbia, 19–22 October 2014. Paper No. 165–11.

Bandy, M.C. (1938): Mineralogy of three sulphate deposits of northern Chile. *Am. Mineral.*, **23**, 669–760.

Brandenburg, K. & Putz, H. (2005): *DIAMOND* Version 3. Crystal Impact GbR. Bonn, Germany.

Brown, I.D. & Altermatt, D. (1985): Bond-valence parameters obtained from a systematic analysis of the inorganic crystal structure database. *Acta Cryst. B*, **41**, 244–247.

Brugger, J., Bonin, M., Schenk, K.J., Miesser, N., Berlepsch, P., Ragu, A. (1999): Description and crystal structure of nabiasite, $BaMn_9[(V,As)O_4]_6(OH)_2$, a new mineral from the central Pyrénées (France). *Eur. J. Mineral.*, **11**, 879–890.

Buckby, T., Black, S., Coleman, M.L., Hodson, M.E. (2003): Fe-sulphate-rich evaporative mineral precipitates from the Río Tinto, southwest Spain. *Mineral. Mag.*, **67**, 263–278.

Buerger, M.J., Dollase, W.A., Garaycochea-Wittke, I. (1967): The structure and composition of the mineral pharmacosiderite. *Z. Krist.*, **125**, 92–108.

Chukanov, N.V., Chukanov, N.V., Krivovichev, S.V., Chernyatieva, A.P., Möhn, G., Pekov, I.V., Belakovskiy, D.I., Van, K.V., Lorenz, J.A. (2013): Vendidaite, $Al_2(SO_4)(OH)_3Cl{\cdot}6H_2O$, a new mineral from La Vendida copper mine, Antofagasta region, Chile. *Can. Mineral.*, **51**, 559–568.

Chukanov, N.V., Aksenov, S.M., Rastsvetaeva, R.K., Pekov, I.V., Belakovskiy, D.I., Britvin, S.N. (2015): Möhnite, $(NH_4)K_2Na(SO_4)_2$, a new guano mineral from Pabellón de Pica, Chile. *Miner. Petrol.*, **109**, 643–648.

Chukanov, N.V., Aksenov, S.M., Rastsvetaeva, R.K., Möhn, G., Belakovskiy, D.I., Lorenz, J.A. (2016): Riotintoite, IMA 2015-085. CNMNC Newsletter No. 29, February 2016, page 201. *Mineral. Mag.*, **80**, 199–205.

Ciesielczuk, J., Żaba, J., Bzowska, G., Gaidzik, K., Głogowska, M. (2013): Sulphate efflorescences at the geyser near Pinchollo, southern Peru. *J. South Amer. Earth Sci.*, **42**, 186–193.

Ertl, A., Dyar, M.D., Hughes, J.H., Brandstatter, F., Gunter, M.E., Prem, M., Peterson, R.C. (2008): Pertlikite, a new tetragonal Mg-rich member of the voltaite group from Madeni Zakh, Iran. *Can. Mineral.*, **46**, 661–669.

Griffen, D.T. & Ribbe, P.H. (1979): Distortions in the tetrahedral oxyanions of crystalline substance. *N. Jb. Mineral. Abh.*, **137**, 83–91.

Hariya, Y. & Kimura, M. (1978): Optical anomaly garnet and its stability field at high pressures and temperatures. *J. Fac. Sci*, **18**, 611–624.

Hawthorne, F.C., Krivovichev, S.V., Burns, P.C. (2000): Crystal chemistry of sulfate minerals. *Rev. Mineral. Geochem.*, **40**, 1–112.

Howell, D. (2012): Strain-induced birefringence in natural diamond: a review. *Eur. J. Mineral.*, **24**, 575–585.

Ibers, J.A. & Hamilton, W.C., Eds (1974): International Tables for X-ray Crystallography. Vol. **IV**, The Kynoch Press, Birmingham, UK.

Jambor, J.L., Nordstrom, D.K., Alpers, C.N. (2000): Metal-sulfate salts from sulfide mineral oxidation. *Rev. Mineral. Geochem.*, **40**, 303–350.

Kampf, A.R., Mills, S.J., Housley, R.M., Williams, P.A., Dini, M. (2012): Alcaparrosaite, $K_3Ti^{4+}Fe^{3+}(SO_4)_4O(H_2O)_2$, a new hydrophobic Ti^{4+} sulfate from Alcaparrosa, Chile. *Mineral. Mag.*, **76**, 851–861.

Kampf, A.R., Mills, S.J., Nash, B.P., Housley, R.M., Rossman, G. R., Dini, M., Gatta, G.D. (2013): Camaronesite, $[Fe^{3+}(H_2O)_2(PO_3OH)]_2(SO_4){\cdot}1\text{–}2H_2O$, a new phosphate-sulfate from the Camarones Valley, Chile, structurally related to taranakite. *Mineral. Mag.*, **77**, 453–465.

Libowitzky, E. (1994): Optical anisotropy in the spinel group: a polishing effect. *Eur. J. Mineral.*, **6**, 187–194.

Liebau, F. (2003): Ordered microporous and mesoporous materials with inorganic hosts: definitions of terms, formula notation and systematic classification. *Micropor. Mesopor. Mater.*, **58**, 15–72.

Long, G.J., Longworth, G., Day, P., Beveridge, D. (1980): A Mössbauer-effect study of the electronic and magnetic properties of voltaite, a mixed-valence mineral. *Inorg. Chem.*, **19**, 821–829.

Majzlan, J., Alpers, C.N., Koch, C.B., McCleskey, R.B., Myneni, S.C.B., Neil, J.M. (2011): Vibrational, X-ray absorption, and Mössbauer spectra of sulfate minerals from the weathered massive sulfide deposit at Iron Mountain, California. *Chem. Geol.*, **284**, 296–305.

Majzlan, J., Schlicht, H., Wierzbicka-Wieczorek, M., Giester, G., Pöllmann, H., Brömme, B., Doyle, S., Buth, G., Bender Koch, C. (2013): A contribution to the crystal chemistry of the voltaite group: solid solutions, Mössbauer and infrared spectra, and anomalous anisotropy. *Mineral. Petrol.*, **107**, 221–233.

Marschik, R. & Fontboté, L. (2001): The Punta del Cobre Formation, Punta del Cobre–Candelaria area, northern Chile. *J. South Amer. Earth Sci.*, **14**, 401–433.

Matsnev, M.E. & Rusakov, V.S. (2012): SpectrRelax: An application for Mössbauer spectra modeling and fitting. *Proc. AIP Conf.*, **1489**, 178–185.

McAloon, B.P. & Hofmeister, A.M. (1993): Single-crystal absorption and reflection infrared spectroscopy of birefringent grossular-andradite garnets. *Am. Mineral.*, **78**, 957–967.

McCusker, L. (2005): IUPAC nomenclature for ordered microporous and mesoporous materials and its application to non-zeolite microporous mineral phases. *Rev. Mineral. Geochem.*, **57**, 1–16.

Mereiter, K. (1972): Die Kristallstruktur des Voltaits, $K_2Fe^{2+}{}_5Fe^{3+}{}_3Al(SO_4)_{12}\square 18H_2O$. *Tschermaks Mineral. Petrogr. Mitt.*, **18**, 185–202.

Nestola, F., Cámara, F., Chukanov, N.V., Atencio, D., Coutinho, J. M.V., Contreira, R.R., Filho, F.G. (2012): Witzkeite: a new rare nitrate-sulphate mineral from a guano deposit at Punta de Lobos, Chile. *Am. Mineral.*, **97**, 1783–1787.

Palache, C., Berman, H., Frondel, C. (1951): The System of Mineralogy. Seventh ed. Vol. **2**, John Wiley and Sons Inc, New York.

Petříček, V., Dušek, M., Palatinus, L. (2006): Jana2006. Structure determination software programs. Institute of Physics, Praha, Czech Republic.

Romero, A., González, I., Galán, E. (2006): The role of efflorescent sulfates in the storage of trace elements in stream waters polluted by acid mine-drainage: The case of Peña del Hierro, Southwestern Spain. *Can. Mineral.*, **44**, 1431–1446.

Sakurai, K., Kato, A., Fujiyama, I., Imayoshi, T. (1958): Voltaite from Konomai mine, Hokkaido. *J. Mineral. Soc. Japan*, **3**, 777–781.

Shtukenberg, A. & Punin, Y.O.B. (2007): Optically Anomalous Crystals. the Netherlands: Springer, Dordrecht, 279 p.

Szakáll, S., Sajó, I., Fehér, B., Bigi, S. (2012): Ammoniomagnesiovoltaite, a new voltaite-related mineral species from Pécs-Vasas, Hungary. *Can. Mineral.*, **50**, 65–72.

Tosca, N.J. & McLennan, S.M. (2009): Experimental constraints on the evaporation of partially oxidized acid-sulfate waters at the martian surface. *Geochim. Cosmochim. Acta*, **73**, 1205–1222.

Wanmao, L., Chen, G., Sun, S. (1987): Zincovoltaite – a new sulfate mineral. *Acta Mineral. Sinica*, **7**, 307–312. in Chinese with English abstract.

Received 2 March 2016
Modified version received 19 April 2016
Accepted 27 April 2016